ELSEVIER

Biophysical Chemistry 64 (1997) 211–224

Biophysical Chemistry

Experimental measurement of the effective dielectric in the hydrophobic core of a protein

Bertrand García-Moreno E. [a,*], John J. Dwyer [a,b], Apostolos G. Gittis [c], Eaton E. Lattman [c,1], Daniel S. Spencer [d], Wesley E. Stites [d]

[a] *Department of Biophysics, Johns Hopkins University, 3400 N. Charles St., Baltimore, MD 21218, USA*
[b] *Intercampus Program in Molecular Biophysics, Johns Hopkins University, Baltimore, MD, USA*
[c] *Department of Biophysics and Biophysical Chemistry, Johns Hopkins University School of Medicine, Baltimore, MD, USA*
[d] *Department of Chemistry and Biochemistry, University of Arkansas, Fayetteville, AR, USA*

Received 30 August 1996; accepted 13 September 1996

Abstract

The dielectric inside a protein is a key physical determinant of the magnitude of electrostatic interactions in proteins. We have measured this dielectric phenomenologically, in terms of the dielectric that needs to be used with the Born equation in order to reproduce the observed pK_a shifts induced by burial of an ionizable group in the hydrophobic core of a protein. Mutants of staphylococcal nuclease with a buried lysine residue at position 66 were engineered for this purpose. The pK_a values of buried lysines were measured by difference potentiometry. The extent of coupling between the pK_a and the global stability of the protein was evaluated by measuring pK_a values in hyperstable forms of nuclease engineered to be 3.3 or 6.5 kcal mol^{-1} more stable than the wild type. The crystallographic structure of one mutant was determined to describe the environment of the buried lysine. The dielectrics that were measured range from 10 to 12. Published pK_a values of buried ionizable residues in other proteins were analyzed in a similar fashion and the dielectrics obtained from these values are consistent with the ones measured in nuclease. These results argue strongly against the prevalent use of dielectrics of 4 or lower to describe the dielectric effect inside a protein in structure-based calculations of electrostatic energies with continuum dielectric models.

Keywords: Buried ionizable group; Dielectric inside a protein; Effective dielectric; Electrostatics; pK_a in hydrophobic environment; Hydration

1. Introduction

The dielectric inside a protein (D_{prot}) is much lower than the dielectric of the surrounding aqueous medium (D_{H_2O}). The dielectric of liquid water is high primarily because water is a liquid and because it has a high density of dipoles. In contrast, the inside of a protein has a high density of apolar atoms, stabilized as clusters sequestered from solvent by the hydrophobic effect, and the polar groups that are buried are always tethered in a semi-rigid orientation and are partially neutralized by hydrogen bonding [1]. Many structural features and physical

* Corresponding author. E-mail: bertran@gibbs.bph.jhu.edu.
[1] Also corresponding author.

0301-4622/97/$17.00 Copyright © 1997 Elsevier Science B.V. All rights reserved.
PII S0301-4622(96)02238-7

properties of proteins are determined directly by the low dielectric inside the protein. For example, most ionizable side chains migrate towards the surface of a protein during the folding process to avoid the seriously destabilizing energetic consequences of becoming trapped in the nascent low dielectric environment [2]. The low dielectric inside a protein is also known to determine functionally essential electrostatic properties of proteins. The redox potentials of proteins involved in electron transfer reactions are tuned partly by the dielectric environment of the reactive metals embedded inside the protein [3]. Similarly, the low dielectric inside a protein prevents autoxidation of the metal atoms in heme proteins [4], influences the pK_a of groups involved in proton transfer reactions in visual pigments [5], and determines the magnitude of the electrostatic interactions at active sites in all enzymes [6,7].

D_{prot} is the most critical parameter used in structure-based calculations of electrostatic effects in proteins with continuum dielectric models [8,9]. It is usually assigned a value between 1 and 4, which presumably reflects the similarity in composition of the interior of a protein to hydrocarbons or to solid polyamides ([10,11] and references therein). The increasingly important role of structure-based calculations in bridging the gap between energetic and structural properties of proteins warrants the systematic experimental examination of the magnitude and character of the dielectric inside proteins.

Direct experimental determination of D_{prot} is practically impossible. Measurements in dry powders and films of peptides and proteins by conventional electrometric methods usually yield values of 1–5 [11–13]. However, the physical meaning of dielectrics measured with dried polypeptides and proteins is very difficult to interpret owing to the lack of information about the conformational and physical states of the macromolecules. Theoretical calculations of D_{prot} have also been attempted. Gilson and Honig predicted low values of 2.5–4.0 based on Kirkwood–Fröhlich dielectric theory applied to a generic set of alpha helices with dipole density similar to that of proteins [11]. Similar values between 1 and 5 have been estimated more recently in actual proteins with theoretical models that account explicitly for the contributions to the dielectric by electron polarization and by dipole relaxation [14,15].

One way to bypass the difficulty in experimental determination of D_{prot} is to measure operational dielectrics (D_{eff}) from the energetics of charged groups in proteins [16]. Phenomenological dielectric constants have been obtained previously from analysis of the Gibbs free energy of interaction between pairs of surface charges [17,18], or between a surface charge and a charge buried in the hydrophobic core of a protein [19]. The D_{eff} values obtained in this way are usually around 50. Presumably they reflect significant contributions from the dielectric of the solvent.

The most reliable estimates of D_{prot} that are experimentally accessible are probably those of D_{eff} obtained by the analysis of the shifts in pK_a experienced by ionizable groups when they are buried in proteins [20,21]. Charged groups buried in hydrophobic locations without a mechanism for charge compensation are particularly useful probes of the dielectric. D_{eff} values were measured in this study from the pK_a shifts of buried lysines in staphylococcal nuclease. These measurements are an extension of earlier work by Stites et al. [20]. These authors demonstrated crystallographically that a lysine substituting for valine-66 in staphylococcal nuclease could be accommodated without structural changes in the hydrophobic core of the protein when the lysine side chain was uncharged. In addition, they measured the shift in pK_a of the buried lysine by analysis of the pH dependence of denaturation of the V66K mutant. The D_{eff} calculated from this shift in pK_a is 12.0.

In the present study we have shown that this D_{eff} is only weakly coupled to the global stability of nuclease, thereby demonstrating that the values of D_{eff} measured in this system can be interpreted in terms of local dielectric effects. This was accomplished by measuring the pK_a values of K66 in two forms of staphylococcal nuclease engineered to have 3.3 and 6.5 kcal mol^{-1} of enhanced stability relative to the wild type. The structure of one of these hyperstable mutants was also determined crystallographically to demonstrate that the ionizable side chain in the uncharged state is in fact buried in the hydrophobic core of the protein. Published pK_a values of groups buried inside other proteins were similarly analyzed in terms of the phenomenological dielectric constants required to account for measured

pK_a shifts. All values of D_{eff} obtained in this way are larger than 10. The values of D_{eff} measured in the nuclease system are the lowest measured thus far, and they might approach the limiting lower value that D_{eff} can assume. The D_{eff} values measured experimentally are invaluable, for they represent the values that have to be reproduced by computational algorithms that attempt to simulate electrostatic interactions in proteins faithful to the behavior that is observed experimentally. The differences between the operational D_{eff} values determined experimentally and the D_{prot} predicted from theoretical considerations with microscopic models suggest the need for further refinements in the computational treatment of dielectrics. The plausible physical origins of these differences and their implications for the structural and functional energetics of proteins will be discussed.

2. Materials and methods

2.1. Materials

Four mutants of nuclease were studied: (1) PHS nuclease, a hyperstable form of nuclease made with a nuclease gene that has three stabilizing mutations, P117G, H124L, and S128A; (2) PHS-V66K nuclease, made with the PHS nuclease gene with lysine substituting for Val-66; (3) Δ + PHS nuclease, another hyperstable nuclease made with a gene with a 44–49 deletion and G50F and V51N mutations, in addition to the mutations already present in the PHS gene; and (4) Δ + PHS-V66K, where the V66K mutation has been introduced into the Δ + PHS background. The lysine substitutions for Val-66 were prepared by the method of Kunkel [22,23] as described previously [24]. The clones of Δ + PHS and Δ + PHS-V66K nuclease were prepared by Dr. Susan Green and Prof. David Shortle at the Johns Hopkins University School of Medicine.

Δ + PHS and Δ + PHS-V66K nuclease were expressed and purified following the procedure described previously by Shortle and Meeker [25]. PHS and PHS-V66K proteins were expressed with a slightly modified procedure [24]. Nuclease was determined to be > 98% pure by SDS-PAGE. Protein concentrations were determined at 280 nm using an optical density of 0.93 [26].

2.2. Determination of protein stability and pH denaturation profiles

The stabilities of the proteins were characterized by guanidine hydrochloride denaturation with protein concentration of 50 μg ml^{-1} at 20°C in 100 mM NaCl + 25 mM sodium phosphate, pH 7.0, using the fluorescence of the single tryptophan at position 140 as a probe of structure, as described previously [24,27]. Data analysis was carried out with previously published procedures [27,28] assuming a two-state model for reversible denaturation. The acid and base denaturation of nuclease monitored by fluorescence was carried out as described previously [27]. No attempts were made to interpret the acid and base denaturation data quantitatively.

2.3. Measurement of proton titration curves

The measurement of proton titration curves was done according to the method developed by Bolen and co-workers [29,30]. Titration curves were measured at 25°C in a thermostatted Radiometer TTA 80 titration apparatus under a CO_2-free N_2 atmosphere. All solutions used during the titration were degassed extensively to avoid contamination with CO_2. A 3 ml portion of protein solution at a protein concentration of approximately 1.15 mg ml^{-1} was used in every titration experiment. The ionic strength was adjusted to 0.10 M with concentrated KCl. The samples were titrated with 0.02 N HCl and 0.02 N NaOH (Fisher, NBS certified reagents) previously calibrated against 1 mM imidazole (Sigma). Titrant was delivered in 5 μl increments with a Brinkmann model 665 Dosimat. The pH was recorded with a Radiometer PHM 95 pH meter using separate glass electrode (pH201, Radiometer) and calomel reference electrode (Ref401, Radiometer). The chain of electrodes was calibrated with NBS certified standard calibration buffers (Radiometer). After the addition of titrant, the pH was recorded when the pH reading met the stability criterion of changes in pH smaller than 20 milli-pH units per minute.

A proton titration curve represents the number of moles of protons bound or released per mole of

protein as the pH is changed. The number of protons reacted with the protein is calculated from the difference between the titration of the protein solution and the titration of a water sample identical in all respects to the protein solution except for the absence of protein. For purposes of quantitation and representation, the titration curves of nuclease and its mutants were fitted with 7th, 8th, or 9th order polynomials by nonlinear least squares.

The proton titration curves of each of the proteins studied were measured at least three times. In general, reproducibility was excellent, especially in the pH region of interest. All titrations were started at the arbitrarily chosen pH of 9. Reversibility was determined routinely by comparison of acid and base titrations of the same sample. The backward and forward titration curves are nearly always superimposable as long as the nuclease is not exposed to extremely acidic or extremely basic pH. Over the narrow range of protein concentration that can be used in these titration measurements (0.5–10 mg ml^{-1}) the titration curves were found to be almost independent of protein concentration.

2.4. Direct measurement of the pK_a of Lys-66 by potentiometry

pK_a values of the buried lysine 66 were determined in the PHS and in the Δ + PHS nucleases by analysis of the difference titration curve obtained by subtracting the polynomial fits of the titration curve of the appropriate background protein from those of the titration curve of the protein bearing the V66K mutation. The difference titration curve reflects the titration of the K66 moiety and also the difference titration of all other ionizable groups that are affected by the mutation at position 66. To demonstrate that in general the difference titration curve is in fact dominated by the titration of the ionizable residue that is removed or incorporated into a protein, the pK_a values that were obtained for the four histidines from the analysis of difference titration curves with Ala-to-His mutants were compared with the values measured by H-NMR in wild type protein ([31], Fitch, Dwyer and García-Moreno, unpublished). The agreement was excellent (data not shown). In addition, we have demonstrated that the titration of mutants of PHS nuclease where V66 has been substituted by residues that do not become ionized in the pH range between 3 and 9 is identical to the titration of the PHS background, indicating that the pK_a values of the ionizable groups in nuclease are not sensitive to the mutations at position 66. This is consistent with the striking similarities that have been found between the crystallographic structures of background and V66K mutant nucleases at neutral pH values.

The analysis of the difference titration curves to obtain pK_a values for K66 is not straightforward. Exact theories for site-specific binding exist [32] but, owing to the large number of binding sites that can potentially be involved, the rigorous application of these theories is not practical. Instead, the difference titration curves were analyzed phenomenologically. pK_a values were obtained by nonlinear least squares fitting of the difference titration curves with a function that describes the difference in the number of hydrogen ions bound to the background and to the V66K protein ($\Delta\nu_i$) in terms of a sum of binding isotherms, each one modified to include a Hill coefficient, as described by Markley [33]:

$$\Delta\nu_i = \frac{10^{n(\mathrm{pH}-\mathrm{p}K_a)}}{1 + 10^{n(\mathrm{pH}-\mathrm{p}K_a)}} \quad (1)$$

Identical pK_a values could also be obtained with other phenomenological functions, such as a sum of binding isotherms modified by a parameter allowing for the scaling of the amplitude of each isotherm. These functions have no physical basis and their general use should be discouraged. However, as discussed later, the exact value of the observed pK_a is not critical for purposes of interpretation of pK_a values in terms of D_{eff}. The agreement between the pK_a of K66 measured directly, by difference potentiometry and, indirectly, by the analysis of the pH dependence of the free energy of denaturation of the wild type and mutant proteins demonstrates the equivalence of these two methods for studying proton-linked phenomena at the level of individual sites.

2.5. Crystallography of Δ + PHS-V66K staphylococcal nuclease

Δ + PHS-V66K was crystallized using the vapor diffusion method at pH 8.0 in 59–61% (vol/vol)

2-methyl-2,4-pentanediol (MPD) and 10.5 mM potassium phosphate buffer. The protein concentration was 16 mg ml^{-1}. Crystals appeared in 8–10 weeks at 4°C. Data were collected for a single crystal with an R-AXIS IIc image plate detector. The crystal was placed in a thin loop, with the crystallization buffer as a cryosolvent, and flash frozen under a steady stream of nitrogen at −178°C. The crystals were found to be isomorphous with those of the uncomplexed wild type protein [34], and this structure was used as an initial model (accession number 1stn in the Brookhaven Protein Data Bank). Valine-66 and the five point mutations in Δ + PHS were modeled as glycine to avoid biasing the side chain conformation. Residues 44–49 were deleted from the model and residues 43 and 50 were connected with a peptide bond. Refinement was carried out using the program XPLOR [35] over the resolution range 6.5–2.1 Å. The side chain coordinates of the lysine, and of the other point mutations, were built into the observed density using the program CHAIN.

3. The pK_a of Lys-66 when buried in the hydrophobic core of nuclease

The pK_a of K66 has been measured previously in the wild type background of nuclease by analysis of the pH dependence of denaturation of wild type and V66K proteins [20]. This required fitting Eq. (2) to the Gibbs free energy of denaturation of wild type and mutant protein measured by guanidine denaturation as a function of pH

$$\Delta\Delta G(\mathrm{pH}) = \Delta\Delta G^{c} - RT \ln \frac{1 + e^{2.303(pK_a^D - \mathrm{pH})}}{1 + e^{2.303(pK_a^N - \mathrm{pH})}} \quad (2)$$

In this expression $\Delta\Delta G(\mathrm{pH})$ represents the (pH-dependent) difference in the Gibbs free energy of denaturation of mutant and wild type protein referenced to an arbitrary pH, $\Delta\Delta G^{c}$ is the free energy of denaturation from which the pH dependence of the Lys-66 has been separated, and pK_a^D and pK_a^N refer to the pK_a of K66 in the denatured and in the native states respectively. The pK_a^N value of K66 in the wild type background that was resolved by this method is 6.38 (±0.37) or less (Table 1). This pK_a value is only a limit; it was difficult to determine the number more accurately owing to the marginal stability of the V66K mutant.

Table 1
pK_a of Lys-66 in three staphylococcal nuclease backgrounds

Protein	ΔG_{H_2O} / (kcal mol^{-1}) [a]	pK_a	D_{eff} [b]
Wild type	5.5	–	–
V66K	−1.6 [c]	≤ 6.38 ± 0.37	12.1
PHS	8.8	–	–
PHS-V66K	1.4	6.35 ± 0.10	12.1
Δ + PHS	12.0 [d]	–	–
Δ + PHS-V66K	4.9 [d]	5.76 ± 0.30	10.7

[a] Free energies were measured at 20°C, pH 7.5, and 0.125 M ionic strength.
[b] Calculated according to Eq. (3).
[c] Data from [20].
[d] Data by S. Green and D. Shortle (unpublished).

The difference potentiometric method is a faster, direct, more convenient method for measuring phenomenological pK_a values. The potentiometric experiment is most accurate when the protein remains in the folded conformation at least through part of the pH range of titration. V66K nuclease is only marginally stable ($\Delta G_{H2O} = -1.6$ kcal mol^{-1} at pH 7.0, and 0.0 kcal mol^{-1} at pH 9); it was therefore not possible to measure the pK_a of K66 in the wild type background by difference potentiometry. The hyperstable PHS and Δ + PHS nucleases, however, were well suited for measurements with the potentiometric method. One of the advantages of the direct potentiometric determination of pK_a values is that it avoids potential pitfalls in the analysis with Eq. (2), where the pK_a of interest, pK_a^N, is statistically correlated with $\Delta\Delta G^{c}$ [20].

The hydrogen ion titration curves of PHS and of PHS-V66K are shown in Fig. 1. Data from multiple titration experiments are included in the titration curve for each of the proteins. The difference titration curves of the K66 mutation in the PHS and in the Δ + PHS backgrounds are depicted in Fig. 2. It is evident from the quality of these data that the difference potentiometric method can be used successfully to resolve the titration behavior of individual residues. The identity of the groups that contribute to the difference potentiometric curves can

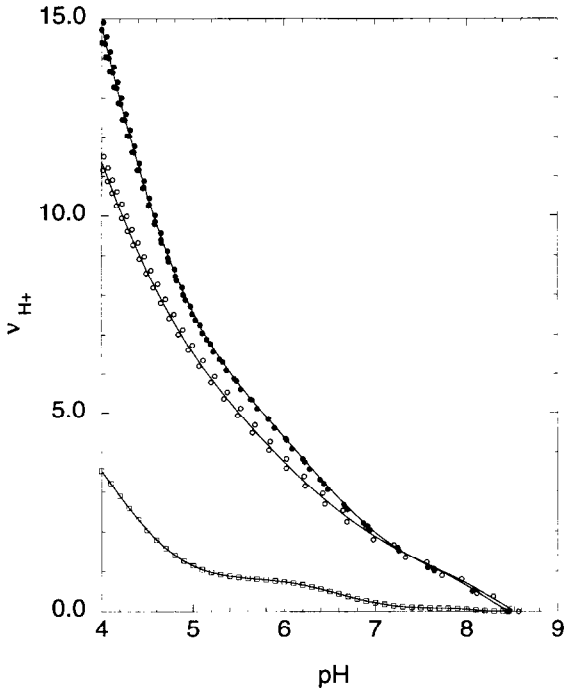

Fig. 1. Potentiometric titration curve of PHS staphylococcal nuclease (filled circles) and of the PHS-V66K mutant (open circles), measured at 25°C, in 100 mM KCl. The lines depict the fits of eighth order polynomials through the experimental points. The difference titration curve is shown at the bottom of the figure (open squares).

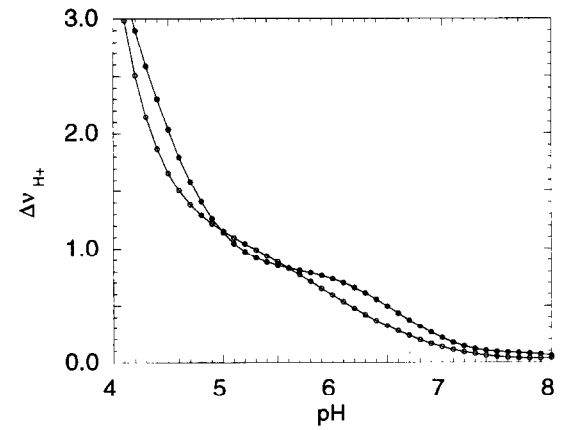

Fig. 2. Difference titration curves representing the ionization of K66 in PHS (filled circles) and in Δ + PHS (open circles) staphylococcal nucleases at 25°C, 100 mM KCl.

only be inferred. However, several independent lines of evidence strongly suggest that the segment of the difference titration curves between pH 5 and 7 represents the ionization of the buried K66. First, the difference titration curve of other mutants of nuclease with substitutions at position 66 that do not titrate in the pH range 3–9 are perfectly flat in this pH range. Second, the stability of the folded conformation is coupled to the ionization of the buried K66, as discussed below, and the ionization events detected by the potentiometric titration track with the conformational change detected by fluorescence. Finally, with His-to-Ala mutants of nuclease we have demonstrated, by comparing pK_a values measured by H-NMR and by analysis of differential titration curves, that in general the shape and amplitude of the difference titration curve are dominated by the ionization of the group that is removed from the background protein and not by the electrostatic or conformational coupling of the mutation to other ionizable groups (Fitch, Dwyer and García-Moreno, unpublished).

The close similarities between the three-dimensional structures of the wild type and of the K66 mutants at neutral pH also support the idea that the titrations obtained by difference potentiometry reflect primarily the ionization of the lysine that was introduced into the background protein. The other ionizable groups that could, in principle, contribute to the difference titration curve are those that titrate with pK_a values close to the pK_a values measured for K66. These groups are His-8, His-46, His-121, His-124, and the amino terminus. His-124 is absent in the PHS mutant, and both 124 and 46 are absent in the Δ + PHS mutant. The pK_a values of the histidines measured in wild type nuclease by H-NMR are: $pK_a = 6.73$ for His-8, $pK_a = 5.89$ for His-46, $pK_a = 5.54$ for His-121, and $pK_a = 5.92$ for His-124 [36]. The pK_a of the amino terminus has not been measured. However, the five amino terminal residues in this protein are disorganized and invisible in the crystal structure, therefore the pK_a of the amino terminus is probably identical in the background and in the K66 protein. Similarly, His-8 and His-46 are solvent exposed and unlikely to be affected by the mutation at position 66. Furthermore, the pK_a of His-8 is already close to the pK_a values of histidines in model compounds. It is also unlikely that His-121

contributes significantly to the difference titration curve, as its pK_a value is not normalized to model compound values even under denaturing conditions (Fitch, Dwyer and García-Moreno, unpublished).

The difference titration curves in both the PHS and the Δ + PHS systems suggest that the protonation of the buried K66 destabilizes the protein severely. This can be appreciated from the curves in Fig. 2 by the sudden uptake of protons that is observed in the acid limit of the difference titration curve. This proton uptake signals the onset of acid denaturation. It reflects the normalization of pK_a values of carboxylic acids in the denatured state, and is a characteristic signature of denaturation observed by the proton titration curves. The coupling between the ionization of K66 and the stability of the protein was also studied directly by pH-induced denaturation monitored by fluorescence. The acid-induced and base-induced denaturation of wild type, PHS, and PHS-V66K nuclease is described by the data in Fig. 3. From the comparison between the acid denaturation profile of PHS and PHS-V66K it can be concluded unequivocally that the stability of the V66K mutant is coupled, albeit weakly, to the titration of the buried lysine. The acid branch of the denaturation curve for PHS-V66K in Fig. 3 is biphasic, and the midpoint of the denaturational transition is at pH 5.4, which corresponds to the plateau observed in the acid limit of the titration of K66 observed in the difference denaturation curve for K66 in the PHS background, shown in Figs. 1 and 2. This suggests that approximately half of the protein molecules are still folded after K66 is fully protonated. Whether or not the positively charged side chain remains buried in the folded protein is not known. These data do suggest, however, that the lower limit of the pK_a of K66 in the PHS protein is determined not by the pH of denaturation of the protein itself, but by the effects of the protein matrix on the self energy of the charged form of K66.

The pK_a values of K66 obtained by fitting the difference titration curves with Eq. (1) are listed in Table 1. Notice that the pK_a values measured potentiometrically in the hyperstable PHS and Δ + PHS proteins are comparable to the pK_a values measured in the wild type background by analysis of the pH dependence of the denaturation free energy. The apparent error in the pK_a of K66 in the PHS background is small and of the same magnitude as errors of pK_a values measured by analysis of H-NMR titrations also with the Hill equation (Eq. (1)). The error in the pK_a values measured in the more stable Δ + PHS background is considerably larger, perhaps because of the small contributions of other titratable groups whose pK_a values are affected by the V66K mutation, as reflected by the abnormal shape and amplitude of this titration curve. It is important to warn against overinterpretation of the pK_a values listed in Table 1. Although visual inspection of the difference titration curves will confirm that these pK_a values describe the titration event centered near pH 6, these pK_a values were obtained by analysis of the titration data with a phenomenological function that lacks a solid physical basis. Therefore the phenomenological pK_a do not represent true pK_a values. As discussed below, the exact value of the pK_a of K66 is not critical for interpretation in terms of D_{eff}.

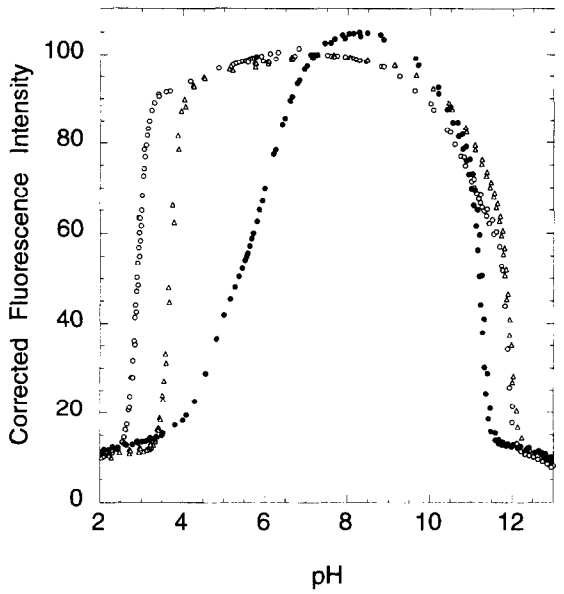

Fig. 3. Acid and base denaturation of wild type (open triangles), PHS (open circles), and PHS-V66K (filled circles) nucleases measured at 20°C. The ionic strength at the beginning of each titration is 125 mM. The denaturation profiles of wild type and PHS nucleases were constructed by superimposing five independent data sets; those of PHS-V66K include four data sets. The precision of each data set is very high, and the high accuracy of the data can be gauged by the fact that the independent data sets are almost superimposable.

The Gibbs free energies of denaturation (ΔG_{H_2O}) of the different mutants of nuclease, measured at pH 7.5, are also listed in Table 1. The PHS form of nuclease is 3.3 kcal mol^{-1} more stable than the wild type, and the Δ + PHS is 3.2 kcal mol^{-1} more stable than the PHS nuclease itself. These stabilizing increases in ΔG_{H_2O} are also reflected in the V66K mutants: PHS-V66K is 3.0 kcal mol^{-1} more stable than the V66K mutant alone, and Δ + PHS-V66K mutant is 3.5 kcal mol^{-1} more stable than PHS-V66K. The increased stability of the PHS is evident from the acid denaturation profiles in Fig. 3. The lower pH for onset of acid denaturation of Δ + PHS, as detected by the upward inflection in the difference titration curves in Fig. 2, reflects its increased stability relative to PHS. The differences in stability between wild type, PHS, and Δ + PHS proteins are only marginally reflected in the pK_a of K66. The pK_a values in the wild type and in the PHS backgrounds are identical, and the difference in pK_a in PHS and in the Δ + PHS backgrounds is 0.59 pK unit, corresponding to 0.80 kcal mol^{-1}. The value of the measured pK_a for K66 is apparently not limited by the acid denaturation of the protein. This marginal coupling between the global stability of the protein and the pK_a of the buried lysine suggests that the pK_a values measured are in fact reporting energetics determined by the local environment of the K66 side chain or by global properties that are not proportional to the total stability of the protein.

Fig. 4. Crystallographic structure of Δ + PHS-V66K staphylococcal nuclease depicted with MolScript [63]. The carbon atoms of the side chain of K66 are represented as shaded spheres, and the location of the NZ atom is identified by the white sphere.

4. Environment of the buried side chain of Lys-66

The useful interpretation of the energetics of ionization in terms of phenomenological dielectric constants requires some knowledge of the environment of the buried side chain. For this reason the structure of the Δ + PHS-V66K mutant was determined crystallographically. Fig. 4 depicts the structure obtained under conditions of pH where the buried K66 is uncharged. The position of the K66 side chain is highlighted. The overall fold of the Δ + PHS-V66K nuclease is the same as the fold of the wild type nuclease. The environment of K66 in the Δ + PHS structure and in the wild type structure that was published previously are indistinguishable [20]. The side chain of K66 is buried in the β barrel domain of nuclease, which has been demonstrated to be the more stable part of the protein and to correspond to its hydrophobic core [37]. The NZ atom is effectively sequestered from solvent, buried deeply inside the protein and ~ 10.6 Å from the nearest water-accessible surface. All the atoms in van der Waals contact with the NZ atom are apolar atoms of the side chains of Val-23, Leu-25, Leu-36, Thr-62, Ile-92, and Val-99. There are only three nitrogen and four oxygen atoms within a 6.4 Å radius of the NZ atom; the closest one is 4.1 Å away and the rest are more than 5 Å away. The distance to the nearest charged atom is 9 Å. The magnitude of the electrostatic potential, calculated at the NZ atom with the linearized Poisson–Boltzmann equation by the method of finite differences at the pH corresponding to the pK_a of K66, is negligible (−0.10 kT, see Table 2). The environment of K66 is very different from that of naturally occurring buried ionizable residues, which usually include charge compensating mechanisms either through hydrogen bonding or ionic interactions [38]. In this respect the ionizable moiety of K66 is unique. It is the best probe available for measuring

Table 2
Structural and energetic parameters of buried ionizable residues in other proteins

Protein	(pdb code)	Residue	ΔpKa [a]	D_{eff} [b]	ψ_{el} (kT) [c]	Nearest charged atom [d]	Depth of burial [e]	No. of polar atoms within 3.6 Å
Staph. nuclease	(2snm)	Lys-66	4.05	12	−0.10	8.80	12.0	0
Lysozyme M102K	(1l54)	Lys-102	3.90 [32]	14	0.88	9.05	7.2	1
Thioredoxin (ox)	(2trx)	Asp-26	3.50 [21]	13	0.66	5.59	0.0	2
Thioredoxin (red)	(3trx)	Asp-26	5.00 [53]	12	−1.82	5.02	0.0	1
Cytochrome *c*	(1hrc)	His-26	3.40 [54]	21	3.00	8.29	3.6	2
Cathepsin	(1huc)	Glu-171	1.00 [55,56]	39	−0.33	8.97	0.0	3
Subtilisin inhibitor	(2ssi)	His-43	3.35 [57]	14	−0.04	8.94	7.4	2
Erabutoxin	(3ebx)	His-6	3.75 [58]	18	2.64	3.40	6.5	0
CEW lysozyme	(2lyz)	Glu-35	1.60 [59]	23	0.67	6.77	5.8	0
Lysozyme Q105E	(1l98)	Glu-105	1.50 [60]	28	−0.13	4.06	0.0	1
Cytochrome *c*	(1hrc)	Prop	> 5.00 [61]	10	–	6.59	10.7	3
Glutathione transf.	(1gst)	His-14	> 2.60 [62]	18	–	4.04	0.0	0

[a] ΔpK_a values were calculated with reference to pK_a values measured in model peptide by H-NMR [8]. These pK_a values are: Arg (12.0), Lys (10.4), His (6.6), Glu (4.5), Asp (4.0), heme propionic acid (4.0).
[b] D_{eff} values were calculated according to Eq. (3).
[c] The electrostatic potential at the titratable atom (ψ_{el}) was computed with the linear Poisson–Boltzmann equation by the method of finite differences with the program DELPHI by Biosym Corp [41]. The potential was computed at the pH corresponding to the observed pK_a. The state of ionization of titratable residues that was used in the calculation of ψ_{el} was computed separately with the modified Tanford–Kirkwood algorithm [8]. The dielectrics of protein and solvent were assigned values of 15 and 78.5 respectively [42,41].
[d] Distance (Å) to the nearest charged atom at the pH equivalent to the observed pK_a.
[e] Approximate distance (Å) between the buried atom and the closest water-accessible surface.

the dielectric effect of the hydrophobic interior of a protein.

5. Values of D_{eff} in nuclease and in other proteins

The pK_a values listed in Table 1 were interpreted in terms of phenomenological dielectric constants (D_{eff}) obtained from the analysis of the shifts in pK_a relative to reference state values in terms of the equation originally proposed by Born to quantitate the hydration free energy of ions [39]:

$$1.359\Delta pK_{ii} = \frac{332}{2r_{cavity}}\left(\frac{1}{D_{eff}} - \frac{1}{D_{H_2O}e^{\kappa r_{cavity}}}\right) \quad (3)$$

In this expression κ is the Debye–Hückel parameter, and the exponential term accounts for ionic strength effects. r_{cavity} refers to the cavity radius of the charged atom; a value of 2.17 Å was used [40]. ΔpK_{ii} refers to the difference in the pK_a values measured in the protein and in model compounds, ΔpK_{obs}, corrected to account for the effects of other charged groups on the observed pK_a according to

$$\Delta pK_{ii} = \Delta pK_{obs} - 0.434 z_i \psi_{el} \quad (4)$$

The pK_a of lysine in the reference state that was used to calculate ΔpK_{obs} is 10.4, the value measured by ^{13}C-NMR in a Gly-Gly-Lys-Gly-Gly pentapeptide [8]. ψ_{el} in Eq. (4) represents the electrostatic potential in units of kT, calculated at the pH of the observed pK_a with the Poisson–Boltzmann equation solved by the method of finite differences [41]. z_i refers to the valence charge of the ionizable group, +1 for basic amino acids and −1 for acidic ones. A value of $D_{prot} = 15$ was used in these calculations, following the recommendations of Antosiewicz et al., who found that in calculations based on the finite difference algorithm this value is necessary to reproduce the titration behavior of buried groups in proteins that is observed experimentally [42,43]. Eq. (4) is not exact but it accounts for most of the coulombic effect on the pK_a values that were measured.

The values of D_{eff} that were obtained from analysis of the energetics of ionization of K66 with Eq. (3) are listed in Table 1. One possible caveat with Eq. (3) is that the predicted D_{eff} values are very sensitive to the value of r_{cavity}, which is a parameter that is particularly difficult to define. Rashin and Honig have demonstrated that Eq. (3) reproduces the energetics of solvation of spherical inorganic ions when the value of r_{cavity} is defined as the radius of the atom that contains a negligible electron density contribution from the surrounding solvent [39]. This concept has been generalized for organic charged molecules [40]. The value of 2.17 Å that was used in the calculations presumably represents the united atom radius of derivatives of ammonium. If values of 1.5 Å, 2.30 Å or 3.17 Å had been used instead, representing cavity radii of other types of nitrogen atoms, the predicted D_{eff} for K66 in PHS would be 16.5, 11.5 and 8.6 respectively. There is also uncertainty in the model compound pK_a values that are used to calculate ΔpK_{obs}. The value of 10.4 that was used represents the expected pK_a of lysines in unfolded proteins. If reference pK_a values of 10.0 or 11.0 had been used instead, the D_{eff} values measured from the pK_a of K66 in PHS nuclease would be 13.2 and 10.7 respectively. Similarly, given the uncertainties in the phenomenological analysis of the difference titration curves in terms of the Hill equation, it is necessary to consider the dependence of D_{eff} on the value of the measured pK_a. If the pK_a were 7.35 instead of 6.35 the predicted D_{eff} would be 16, and if instead the pK_a were 5.35 the D_{eff} would be 10.

Even after allowing for the uncertainties in r_{cavity} and in model compound pK_a values, the values of D_{eff} predicted with Eq. (3) for K66 in PHS range only from 8.6 to 16.5. It is extremely unlikely that Eq. (3) could be used to measure values of D_{eff} that approached the theoretical value of $D_{prot} = 4$. For example, in the case of lysine, a shift of 10.7 pK units would be required to predict a D_{eff} of 5, and it is very unlikely that the native state of even the most robust of proteins could tolerate this destabilization, equivalent to 14.5 kcal mol^{-1} at 25°C, without undergoing a major conformational reorganization. However, it is clear from the curves in Figs. 2 and 3 that the unfolding of nuclease, although it is coupled to the ionization of the buried K66, does not limit the values of D_{eff} that can be measured. The values of D_{eff} that are listed in Table 1 are significantly higher than $D_{eff} = 7$, which is the lowest possible value that could have been measured if the V66K mutation did not alter the sensitivity to acid of the PHS background protein.

In order to establish whether the values of D_{eff} measured by K66 in nuclease are representative of the situation in other proteins, we analyzed the ΔpK_{obs} reported for other buried ionizable groups with Eq. (3). The D_{eff} values are reported in Table 2 along with several structural descriptors, including the depth of burial of the ionizable atom, the number of polar atoms within hydrogen bonding distance, the distance to the nearest charged residue, and the magnitude of the electrostatic potential in that location. Although it is obvious that different values of D_{eff} are reported for different cases, all of the measurements are remarkably consistent with what is observed in nuclease. Most buried ionizable groups report D_{eff} values between 10 and 23 and there does not appear to be significant correlation between the value of D_{eff} and the structural details of the charged atoms' microenvironments, including aspects such as the magnitude of the electrostatic potential at the site, the distance between the buried charged atom and the nearest water-accessible surface, and the presence or absence of polar atoms within hydrogen bonding distance. The values of D_{eff} between 10 and 23 are significantly lower than the values of $D_{eff} = 48$ and higher that have been measured by analysis of the energy of interaction of surface charged groups [17–19]. A few of the D_{eff} values listed in Table 2 are higher than the 10–23 range, but what is particularly significant is that none report D_{eff} values lower than those reported by K66 in nuclease. In this regard, the dielectric response of K66 in nuclease seems to represent a limiting case, and one that is less difficult to interpret than most, owing to the ideal location of the ionizable NZ atom deeply buried in the hydrophobic core of the protein, without any charge compensating mechanisms, perfectly surrounded by apolar matter.

6. Implications and possible origins of $D_{eff} \geq 10$

A dielectric constant is a macroscopic parameter that describes the response of a material to the

presence of a charge. A material with a high dielectric can alter the field of the charge by its presence. Two different microscopic phenomena determine the magnitude of a dielectric: electronic polarizability and dipolar relaxation. The magnitude of the contributions by these two types of effects can be radically different. They can be separated by analysis of the frequency dependence of the dielectric, also referred to as dielectric dispersion. In the high frequency limit the dielectric is determined almost exclusively by electronic polarization. In most polar liquids the value of the high frequency dielectric is low, between 2 and 4, similar to the low dielectric of hydrocarbons such as pentane ($D = 1.8$), propane ($D = 1.6$), pentadiene ($D = 2.3$) and benzene ($D = 2.3$). In contrast, the total dielectric of polar organic liquids such as methylamine ($D = 9.4$), pyridine ($D = 12.3$), octanol ($D = 10.3$) and acetaldehyde ($D = 21$) is higher owing to significant contributions by dipolar relaxation [44]. Evidently, dynamic dipolar relaxation accounts for the majority of the dielectric effect in polar liquids. This is also well illustrated by the comparison of the dielectric of water at room temperature ($D = 78.5$) with its dielectric when frozen under high pressure ($D = 3.0$).

The definition of the dielectric in a protein is not straightforward. Some of the most detailed theoretical estimates of what the dielectric inside a protein should be were calculated with a microscopic model that described elastic electronic polarizabilities with a set of atomic point polarizabilities, and dynamic dipolar reorientation in terms of the low frequency collective modes of vibration described through normal mode analysis [11,14,15]. These calculations were done under the assumption that the polarization inside the protein can be calculated without considering the re-polarization of the protein by the solvent. They predict that the contributions to the dielectric from atomic polarizabilities are uniform throughout the protein, but that contributions from dipolar relaxation can vary greatly in the different regions of the protein. These models predict low values for the dielectric inside the protein ($D_{prot} \leq 5$).

Based on the highly apolar environment surrounding the NZ atom of K66, it would be reasonable to expect that in the absence of significant conformational relaxation D_{eff} should have values comparable with those predicted computationally in proteins, and with those measured experimentally for pure hydrocarbons and solid amines. Instead, the value of D_{eff} inside a protein is high and resembles more the dielectric of liquid amines, alcohols and aldehydes. Even the largest shifts in pK_a induced by transfer of an ionizable group from water into a hydrophobic environment, which have been measured in synthetic polypeptides, do not predict D_{eff} values below 8.5 [45]. The high values of D_{eff} in proteins are consistent with the ideas proposed by Warshel and co-workers, who view the inside of the protein as a medium of high polarity [46,47]. However, at least under conditions where the buried K66 is uncharged, the explanation that the high D_{eff} needed to reproduce observed solvation energies with the Born equation reflects the fact that the charged sites are always found in regions of high polarity does not hold true, as K66 is embedded in a perfectly hydrophobic pocket. It is also unlikely that the high values of D_{eff} can be explained on the basis of the influence of the reaction field of the surrounding solvent, otherwise the magnitude of D_{eff} would probably be dependent on the depth of burial, and that trend is not observed among the cases presented in Table 2.

The high values of D_{eff} might reflect the dynamic properties of proteins. In principle the use of normal mode analysis to approximate the dynamic contributions to the dielectric in theoretical calculations of D_{prot} is valid; the dipoles in a folded protein are constrained with a rigid orientation and cannot realign with the field, and the contribution to the dielectric by dynamic dipolar relaxation should be treated as a small perturbation [14,15]. In practice, however, it is apparent that the normal mode dynamics, which describe dynamics over a few picoseconds, cannot account for slower structural transitions that are accessible in the time scale of the equilibrium experiments used to measure D_{eff} from pK_a shifts. The discrepancy between D_{prot} and D_{eff} is probably related to the underestimation of the contributions by dynamic dipolar relaxation in the calculation of D_{prot}. The structural fluctuations that are being reflected in the magnitude of D_{eff} could be the ones that are monitored by hydrogen isotope exchange in the time scale of minutes [48]. Warshel and co-workers proposed that this might include local unfolding, such that the charged atoms become

exposed to waters or dipoles from the protein that can reorient in response to the electrostatic field [46]. Direct penetration of solvent into the hydrophobic core of a protein could also account for the high values of D_{eff} [48]. The possibility that high values of D_{eff} reflect a reorganization of the peptide dipoles after the buried group becomes ionized cannot be excluded at present, owing to the absence of structural information under conditions of pH where buried groups are ionized. None of the experimental evidence presently available allows the conclusive interpretation of the structural and physical origin of the high values of D_{eff}.

Although D_{eff} is a heuristic parameter defined operationally and without precise physical meaning, in structure-based calculations of electrostatic interactions in proteins with continuum dielectric models it would be valid and appropriate to substitute the commonly used values of $D_{prot} = 1–4$ with values closer to the measured D_{eff}. Use of a high D_{eff} would probably alter the physical microscopic interpretation of the origins of pK_a values and ionization energetics of proteins. To illustrate this point, consider the following. According to Eq. (3) it costs 38 kcal mol^{-1} to move a charged particle from an aqueous medium into a medium with $D = 2$, 7 kcal mol^{-1} if the low dielectric medium has $D = 10$, but only 3 kcal mol^{-1} if $D = 20$. Clearly, the difference between a $D_{prot} = 4$ and a $D_{eff} = 12–20$ is significant and loaded with implications about the magnitude of contribution by hydration of ionizable residues to the stability of folded proteins. Computationally, the problem of computing electrostatic free energies from structure also becomes more tractable when larger dielectrics are used. This has already been demonstrated clearly: in order to predict correctly the ionization energetics of protein with the finite difference solution of the Poisson–Boltzmann equation, it is necessary to use a $D_{prot} = 20$ or higher for interactions between surface ionizable groups and values of $D_{prot} = 15$ for buried residues [42,43,49]. The large values of D_{eff} that are found experimentally also partly explain the surprising success of predictions of the ionization behavior of surface groups with simple models such as the modified Tanford–Kirkwood model pioneered by Gurd. In this model, the dielectrics that are used to calculate the energy of interaction between surface ionizable groups are never less than $(D_{prot} + D_{H20})/2$, reproducing (unwittingly) the effects of large D_{eff}, and compensating partly for the omission of self energy terms in the calculation of pK_a values [8,49].

The data presented in Table 2 suggest that there is some degree of positional independence in the value of D_{prot} as reflected by the D_{eff}. Ten out of twelve cases presented in this table have values of D_{eff} between 10 and 23, and there is no obvious correlation between the value of D_{eff} and the depth to which the ionizable group is buried, or other details of the microenvironment. This is important, as the positional independence of D_{prot} is one of the central assumptions of continuum dielectric models. The other common assumption is that proteins behave as linear dielectric media, that is, proteins are rigid relative to changes in the electrostatic field, and changes in the field are not accompanied by significant changes in the structure. The data in Figs. 2 and 3 do not offer conclusive evidence about the validity of this assumption in the titration of K66 in nuclease. It remains to be verified by the detailed study of the specific structural and physical changes concomitant with the ionization of a buried group.

In general, continuum dielectric models will probably continue to be more useful for structure-based calculation of electrostatic energies and titration properties of proteins than truly microscopic models that attempt to compute the dielectrics directly from structure. This situation will be exacerbated if it turns out that the high values of observed D_{eff} originate from slow structural fluctuations of proteins that are difficult to model with molecular dynamics. On the other hand, molecular dynamics might provide insights about the structural and physical origins of the value of $D_{prot} = 20$ that is necessary to predict correctly the titration of surface ionizable groups. The effect equivalent to $D_{prot} = 20$ might be emulated by identifying multiple conformations through dynamics simulations, and considering contributions by many of them, in some of which charged groups might be more exposed to solvent than in others, in the calculations of pK_a values ([50–52], M. Gilson, personal communication). Systematic studies that define further the phenomenological dielectric constants in proteins and that contribute more detailed insight about their physical and structural origins and about the role of protein dynamics will

be essential for improved and realistic quantitation of electrostatic effects in proteins.

Acknowledgements

The authors gratefully acknowledge Ms. Carolyn Fitch for development of the program used to calculate the depth of burial of an atom in a protein, Dr. Susan Green for the measurement of free energy of denaturation of the Δ + PHS mutants, and Dr. David Shortle for his generous gift of the clones of Δ + PHS mutants.

This work was supported in part by NSF grant MSC 96-00991 to B.G-M.E., NIH grant GM-36358 to E.E.L., and NIH grant GM-52714-01 to W.E.S.

References

[1] G.D. Rose and R. Wolfenden, Annu. Rev. Biophys. Biomol. Struct., 22 (1993) 381.
[2] C.H. Paul, J. Mol. Biol., 155 (1982) 53.
[3] D. Bashford, M. Karplus and G.W. Canters, J. Mol. Biol., 203 (1988) 507.
[4] R. Varadarajan, T.E. Zewert, H.B. Gray and S.G. Boxer, Science, 243 (1989) 69.
[5] M. Engels, K. Gerwert and D. Bashford, Biophys. Chem., 56 (1995) 95.
[6] Y. Li, A. Kuliopulos, A.S. Mildvan and P. Talalay, Biochemistry, 32 (1993) 1816.
[7] L.I. Krishtalik, J. Theor. Biol., 86 (1980) 757.
[8] J.B. Matthew, F.R.N. Gurd, B. García-Moreno E., M.A. Flanagan, K.L. March and S.J. Shire, CRC Crit. Rev. Biochem., 18 (1985) 91.
[9] K.A. Sharp and B. Honig, Annu. Rev. Biophys. Biophys. Chem., 19 (1990) 301.
[10] R. Roxby, Ph.D. Thesis, Duke University, 1970.
[11] M.K. Gilson and B. Honig, Biopolymers, 25 (1986) 2097.
[12] J. Rupley and G. Careri, Adv. Protein Chem., 41 (1991) 37.
[13] R.H. Tredgold and P.N. Hole, Biochim. Biophys. Acta, 443 (1976) 137.
[14] T. Simonson, D. Perahia and G. Bricogne, J. Mol. Biol., 218 (1991) 859.
[15] T. Simonson, D. Perahia and A.T. Brünger, Biophys. J., 59 (1991) 670.
[16] T.L. Hill, J. Chem. Phys., 60 (1956) 253.
[17] M.J.E. Sternberg, F.R.F. Hayes, A.J. Russell, P.G. Thomas and A.R. Fersht, Nature, 330 (1987) 86.
[18] J.B. Matthew, Annu. Rev. Biophys. Biophys. Chem., 14 (1985) 387.
[19] D.C. Rees, J. Mol. Biol., 14 (1980) 323.
[20] W.E. Stites, A.G. Gittis, E.E. Lattman and D. Shortle, J. Mol. Biol., 221 (1991) 7.
[21] K. Langsetmo, J.A. Fuchs and C. Woodward, Biochemistry, 30 (1991) 7603.
[22] T.A. Kunkel, Proc. Natl. Acad. Sci. U.S.A., 82 (1985) 488.
[23] T.A. Kunkel, J.D. Roberts and R.A. Zakour, Methods Enzymol., 154 (1987) 367.
[24] M.P. Byrne, R.L. Manuel, L.G. Lowe and W.E. Stites, Biochemistry, 34 (1995) 13949.
[25] D. Shortle and A.K. Meeker, Biochemistry, 28 (1989) 936.
[26] S. Fuchs, P. Cuatrecasasas and C.B. Anfinsen, J. Biol. Chem., 242 (1967) 4768.
[27] W.E. Stites, M.P. Byrne, J. Aviv, M. Kaplan and P.M. Curtis, Anal. Biochem., 227 (1995) 112.
[28] D. Shortle, W.E. Stites and A.K. Meeker, Biochemistry, 29 (1990) 8041.
[29] D.W. Bolen and M.M. Santoro, Biochemistry, 27 (1988) 8069.
[30] Y. Huang and D.W. Bolen, Methods Enzymol., 259 (1995) 19.
[31] S. Dao-pin, D.E. Anderson, W.A. Baase, F.W. Dahlquist and B.W. Matthews, Biochemistry, 30 (1991) 11521.
[32] E. Di Cera, Thermodynamic Theory of Site-Specific Binding Processes in Biological Macromolecules, Cambridge University Press, Cambridge, 1995.
[33] J.L. Markley, Acc. Chem. Res., 8 (1975) 70.
[34] T.R. Hynes and R.O. Fox, Proteins, 10 (1991) 92.
[35] A.T. Brunger, J. Kuriyan and M. Karplus, Science, 235 (1970) 458.
[36] A.T. Alexandrescu, D.A. Mills, E.L. Ulrich, M. Chinami and J.L. Markley, Biochemistry, 27 (1988) 2158.
[37] D. Shortle, Adv. Protein Chem., 45 (1995) 217.
[38] A.A. Rashin and B. Honig, J. Mol. Biol., 173 (1984) 515.
[39] A.A. Rashin and B. Honig, J. Phys. Chem., 89 (1985) 5588.
[40] A.A. Rashin and K. Namboodiri, J. Phys. Chem., 91 (1987) 6003.
[41] I. Klapper, R. Hagstrom, R. Fine, K. Sharp and B. Honig, Proteins, 1 (1986) 47.
[42] J. Antosiewicz, J.A. McCammon and M.K. Gilson, Biochemistry, 35 (1996) 7819.
[43] J. Antosiewicz, J.A. McCammon and M.K. Gilson, J. Mol. Biol., 238 (1994) 415.
[44] Handbook of Chemistry and Physics, CRC Press, Cleveland, 1975.
[45] D.W. Urry, D.C. Gowda, S. Peng, T.M. Parker, N. Jing and R.D. Harris, Biopolymers, 34 (1993) 889.
[46] G. King, F.S. Lee and A. Warshel, J. Chem. Phys., 95 (1991) 4366.
[47] A. Warshel, J. Åqvist and S. Creighton, Proc. Natl. Acad. Sci. U.S.A., 86 (1989) 5820.
[48] C. Woodward, Trends Biochem. Sci., 18 (1993) 359.
[49] A. Warshel, S.T. Russell and A.K. Churg, Proc. Natl. Acad. Sci. U.S.A., 81 (1984) 4785.
[50] T.J. You and D. Bashford, Biophys. J., 69 (1995) 1721.
[51] J.J. Wendoloski, J.B. Matthew, P.C. Weber and F.R. Salemme, Science, 238 (1987) 794.

[52] J.J. Wendoloski and J.B. Matthew, Proteins, 5 (1989) 313.
[53] N.A. Wilson, E. Barbar, J.A. Fuchs and C. Woodward, Biochemistry, 34 (1995) 8931.
[54] J.S. Cohen, W.R. Fisher and A.N. Schecter, J. Biol. Chem., 249 (1974) 1113.
[55] G.R. Moore and F. Williams, Eur. J. Biochem., 103 (198) 513.
[56] D. Musil, D. Zucic, D. Turk, R.A. Engh, I. Mayr, R. Huber, T. Popovic, V. Turk, T. Towatari, N. Katunuma and W. Bode, EMBO J., 10 (1991) 2321.
[57] S. Fujii, K. Akasaka and H. Hatano, J. Biochem., 88 (1980) 789.
[58] F. Inagaki, T. Miyazawa, H. Hori and N. Tamiya, Eur. J. Biochem., 89 (1978) 433.
[59] M. Inouc, H. Yamada, U. Hashimoto, T. Tasukochi, K. Hamaguchi, T. Miki, T. Horiuchi and T. Imoto, Biochemistry, 31 (1992) 8816.
[60] P. Pjura, L.P. McIntosh, J.A. Wozniak and B.W. Matthews, Proteins, 15 (1993) 401.
[61] R.T. Hartshorn and G.A. Moore, Biochem. J., 258 (1989) 595.
[62] P. Zhang, G.F. Craminski and R.N. Armstrong. J. Biol. Chem., 266 (1991) 19475.
[63] P.J. Kraulis, J. Appl. Crystallogr., 24 (1991) 946.